Journal of Environmental Management 297 (2021) 113434

Contents lists available at ScienceDirect

Journal of Environmental Management

journal homepage: www.elsevier.com/locate/jenvman

Protein corona on biogenic silver nanoparticles provides higher stability and protects cells from toxicity in comparison to chemical nanoparticles

Federico N. Spagnoletti [a,b], Florencia Kronberg [a,c], Cecilia Spedalieri [d], Eliana Munarriz [a,c], Romina Giacometti [a,c,*]

[a] CONICET-Consejo Nacional de Investigaciones Científicas / Instituto de Investigaciones en Biociencias Agrícolas y Ambientales, Avda. San Martín 4453, C1417DSE, Buenos Aires, Argentina
[b] Cátedra de Microbiología, Facultad de Agronomía, Universidad de Buenos Aires, Buenos Aires, Argentina
[c] Cátedra de Bioquímica, Facultad de Agronomía, Universidad de Buenos Aires, Buenos Aires, Argentina
[d] Humboldt Universität zu Berlin, Department of Chemistry, Brook-Taylor-Str. 2, 12489, Berlin, Germany

ARTICLE INFO

Keywords:
Green nanotechnology
Silver nanoparticles
Capping
Proteomics

ABSTRACT

The development of environmentally friendly new procedures for the synthesis of metallic nanoparticles is one of the main goals of nanotechnology. Proteins and enzymes from plants, filamentous fungi, yeast, and bacteria to produce nanoparticles are both valuable and viable alternatives to conventional synthesis of nanomaterials due to their high efficiency and the low cost to scale up and generate large quantities. The aim of this work is to compare biogenic silver nanoparticles (AgNPs) obtained from cell-free filtrates from the fungus *Macrophomina phaseolina* to conventional chemical AgNPs, in biocidal activity and toxicity. Our results show that bio-AgNPs displayed similar bactericidal activity than chemical AgNPs, but less toxicity in the model organism *Caenorhabditis elegans*. We employed biochemical and proteomic techniques to profile the unique surface chemistry of the capping in the bio-AgNPs and therefore to identify the proteins involved in their synthesis and stability. These results not only suggest that the proteins involved in the synthesis of the nanoparticles and corona formation in the bio-AgNPs are responsible for keeping the silver core preserved making them more stable in time, but also masking and protecting eukaryotic cells from metal toxicity.

1. Introduction

Metallic nanoparticles (NPs) display remarkable chemical features, which make them unique materials and more interesting than the bulk-like metals. NPs present small size and a high surface/volume ratio, characteristics that led them to be broadly included in scientific research and product development in areas such as chemical, medical/pharmaceutical, electronical, industrial, agricultural and environmental (Kim et al., 2007; Marambio-Jones and Hoek, 2010). One of the most studied NPs are silver NPs (AgNPs) because of their powerful antimicrobial action against both Gram-negative and Gram-positive bacteria (Gurunathan et al., 2014), viruses and other eukaryotic microorganisms (Gong et al., 2007).

There are different ways to synthesize NPs, such as physical, chemical, and biological approaches. The first two, although being the most used methods, present environmental problems due to the use of harsh conditions, high temperature, pressure, energy and/or hazardous chemicals that lead to risks for both human health and the environment (Salam et al., 2014). In this sense, biological methods bring interesting advantages compared to conventional chemical approaches. Green synthesis methods, using biotechnology and/or living organisms, are environmentally friendly, safe, clean, inexpensive, and still allow the production of NPs with defined sizes and morphology (Ahmad et al., 2019; Bahrulolum et al., 2021; Xiao et al., 2020). Furthermore, another relevant aspect of including biological constituents (plant extracts, fungal or bacterial cell free filtrates) in the NPs production process is that proteins, amino acids, sugars and other molecules act as capping agents to stabilize NPs (Singh et al., 2016; Khoshnamvand et al., 2019; Mohamed et al., 2019; Quinteros et al., 2019; Prajapati and Mondal, 2021). Working with fungi to obtain NPs presents advantages when compared to other biogenic sources; since most fungi have significant growth rates, high biomass production with easy culturing procedures,

* Corresponding author. CONICET-Consejo Nacional de Investigaciones Científicas / Instituto de Investigaciones en Biociencias Agrícolas y Ambientales, Avda. San Martín 4453, C1417DSE, Buenos Aires, Argentina.
E-mail address: rgiacometti@agro.uba.ar (R. Giacometti).

https://doi.org/10.1016/j.jenvman.2021.113434
Received 18 February 2021; Received in revised form 27 July 2021; Accepted 28 July 2021
Available online 13 August 2021

great diversity of extracellular enzymes secretion, and can produce stable NPs with high concentration rates (Akther et al., 2019; Spagnoletti et al., 2019). Furthermore, biogenic NPs are believed to be more suitable for environmental and/or agricultural applications since they present high biocompatibility, mediated by the biomolecules that act as natural stabilizers of NPs, preventing their aggregation over time and giving them a particular additional stabilization (Deepak et al., 2011). Preliminary evidence suggests the positive response of the soil bacterial community structure to biogenic NPs in comparison to metallic salt (Mishra et al., 2020). Thus, the biomolecules in the surface layer that cover the metallic core of the biogenic NPs would ameliorate their interaction with other biomolecules and could improve the interaction with organisms (Deepak et al., 2011; Akther et al., 2019).

The increasing application of NPs in a range of production processes inexorably leads to the enormous release of these NPs into the surrounding environment. Several reports have shown that NPs can enter cells and alter the biochemistry of cells, leading to oxidative damage in organisms (de Souza et al., 2019). Hence, it is important to study the potential toxicity of any new synthesized NPs. In recent times, the use of some model organisms, such as *Caenorhabditis elegans*, has been considered to analyze the biosafety and the ecological risk of NPs (Baas et al., 2018). This nematode can be used as an animal model providing a valuable possibility for researchers to investigate the biological effects of different compounds at early stages in an inexpensive and reproducible way (Hunt et al., 2020). The effects of NPs on *C. elegans* has been studied recently and results suggest that exposure to some types of NPs at certain doses render negative effects in the development, reproduction, immune response, and neuronal function of *C. elegans* (Wu et al., 2019). However, the information about risk assessments of NPs using *C. elegans* unfortunately is scarce. Moreover, to this day there are no studies that analyze the differential effects of biogenic NPs compared to conventional chemical NPs on *C. elegans*.

In a previous study, our group reported a novel technique for the biological synthesis of AgNPs using a cell-free filtrate of the fungus *Macrophomina phaseolina* (Spagnoletti et al., 2019). Synthesized spherical AgNPs showed biocide activity against different bacteria, but no detrimental effect in fungi, yeast cells or soybean seeds was detected (Spagnoletti et al., 2019). Here, experimental work was designed to investigate and compare biogenic AgNPs against chemical AgNPs at biocidal efficacy and toxicity level in *C. elegans*. Through proteomic analysis we describe the corona on biogenic AgNPs and evaluated the involvement of these molecules in the synthesis process, along with their role in modulating the particle stability.

2. Materials and methods

2.1. Green and chemical nanoparticles synthesis

For biogenic AgNPs (bio-AgNPs) synthesis we followed our protocol previously described in Spagnoletti et al. (2019) using the cell free filtrate (CFF) of the fungus *Macrophomina phaseolina*. Briefly, an isolate of the fungus *M. phaseolina* was used as the source of proteins and other biomolecules for NPs biogenesis purposes. First, the strain was cultivated in a liquid medium containing 100 mL of 50 % potato dextrose broth (PDB) in a shaker at 150 rpm in absence of light at 28 °C for 7 days. The harvested mycelia were washed with MilliQ water to exclude remaining sugars from the culture medium. Fungal clean biomass (1 g) was incubated in 100 mL sterile MilliQ water for 72 h at 28 °C with constant orbital shaking at 150 rpm. The exudate was doubly filtered with Whatman paper No. 1 (Whatman, USA). An aqueous 1 mM silver nitrate ($AgNO_3$) solution was added to the cell free filtrate (CFF), and kept the flasks protected of light at 28 °C with shaking up to 72 h (Spagnoletti et al., 2019). Bio-AgNPs were spun down at 10000 rpm for 20 min and washed in MilliQ water. Under the same experimental conditions, flasks with the CFF without the precursor or with MilliQ water in the presence of $AgNO_3$ were used as controls.

For the preparation of chemical AgNPs sodium borohydride ($NaBH_4$) was used to both reduce and to stabilize the NPs (Mulfinger et al., 2007). A 10 mL of 1 mM $AgNO_3$ solution was added dropwise to 30 mL of a 2 mM $NaBH_4$ solution that was chilled at 4 °C. The mixture was stirred on a magnetic stir plate till development of characteristic color.

Synthesis for both chemical and bio-AgNPs was further validated with a UV–vis spectrophotometer (Shimadzu UV-2550, Japan). Study of the NPs morphology was assessed using a Zeiss Supra-40 scanning electron microscope (SEM) with a voltage of 5 kV. Several samples obtained from different batches were analyzed, and 30 images were recorded.

2.2. Bactericidal activity of bio-AgNPs and AgNPs

Bactericidal activity of both synthesized NPs was assessed by liquid growth inhibition test in microtiter plates as described previously in Spagnoletti et al. (2019). Briefly, 10 μL of either bio-AgNPs and chemical AgNPs, at concentrations ranging from 5 to 50 μg/mL were added to 90 μL of a suspension of a mid-log phase culture of *Escherichia coli* strain at 1×10^5 CFU/mL in the LB medium. Experiments were carried out in triplicate. Plates were subjected to orbital shaking at 120 rpm at 37 °C and were read at 600 nm using a Spark20M Multimode Microplate Reader (Tecan, USA) every 2 h up to 24 h. Antibiotic ampicillin (100 μg/mL) was used as the positive control, and bacterial cells in liquid medium without any other treatment as negative control.

Bacterial respiratory activity was analyzed as described in Spagnoletti et al. (2019). Quantification was performed by using the 2,3-bis (2-methoxy-4-nitro-5-sulfo-phenyl)-2H-tetrazolium-5-carboxanilide (XTT) method (Kumar and Poornachandra, 2015). Conversion of XTT by *E. coli* to an orange-colored formazan product was quantified reading absorbance at 490 nm using a Spark20M Multimode Microplate Reader (Tecan, USA). Experiments were carried out in triplicate.

2.3. SDS-PAGE and zymograms analysis

After bio-AgNP synthesis (24 h) the proteins were analyzed by SDS-PAGE electrophoresis. Nanoparticles were precipitated by centrifugation at 10000 rpm for 20 min, washed with MilliQ water, and repeated the process twice. Proteins present in the *M. phaseolina* cell free filtrate (CFF) were concentrated using centrifugal filter units Amicon Ultra-15 of 10 kDa (Millipore). The eluted proteins were then washed with 0.02 M Phosphate-Buffered Saline (PBS) pH 7.5, and concentration was assessed accordingly to Bradford (1976) using the Coomassie Protein Assay reagent (Pierce # 23238).

Sodium dodecyl sulfate-polyacrylamide gels (SDS-PAGE) were prepared as described by Laemmli (1970). Protein samples from CFF and bio-AgNPs (25 μg) were boiled at 100 °C for 10 min in 1 % SDS, followed by centrifugation at 8000 rpm for 10 min for collection of supernatants. Samples and a molecular weight marker (Kaleidoscope, Bio-Rad) were loaded in 10 % SDS-PAGE gels in 1.5 M Tris-HCl pH 8.8 and electrophoresed at 40V for 25 min and later at 100V for 2 h. After electrophoresis, gels were silver stained according to Heukeshoven and Dernick (1985).

Zymograms were assessed by native PAGE and samples (CFF and bio-AgNPs) were applied in non-reducing denaturing loading buffer and were electrophoresed at 50V for 2 h at 4 °C. Afterwards, the gel was soaked in 5 mM guaiacol dissolved in 10 mM sodium acetate buffer, pH 5.6. Gel photographs were taken to document positive activity after 10 min of soaking, till a reddish-brown color appeared where the enzyme/s were located.

2.4. Proteomics

For identification of proteins present in the bio-AgNPs corona and in the CFF from the fungus *M. phaseolina*, samples digestion and Mass Spectrometry (MS) analysis was performed at CEQUIBIEM, Proteomics

Core Facility CEQUIBIEM, at the University of Buenos Aires-CONICET. NanoLC was carried out as previously described (Piccinni et al., 2019). Briefly, samples were exposed to 20 mM dithiotreitol (DTT) for 40 min at 56 °C, and were alkylated with 20 mM Iodoacetamide for 40 min in absence of light and digested with trypsin (Promega V5111) overnight at 37 °C. The extraction of the peptides was carried out with acetonitrile. Samples were lyophilized by Speed Vac and re-suspended with 10 μL of 0.1 % Formic Acid. The samples were separated by nanoLC (EASY-nLC 1000, Thermo Scientific) to then be analyzed by tandem mass spectrometry (spectrometer Q-Exactive, Thermo Scientific) with Orbitrap technology (nano HPLC-ESI-MS/MS). A voltage of 3,5 kV was used for ElectroSpray Ionization (Thermo Scientific, EASY-SPRAY). The MS equipment has a high collision dissociation cell (HCD) for fragmentation and an Orbitrap analyzer (Thermo Scientific, Q-Exactive). XCalibur 3.0.63 (Thermo Scientific) software was used for data acquisition. Q Exactive raw data were processed using Proteome Discoverer software (version 2.1.1.21 Thermo Scientific) and searched against *Macrophomina phaseolina* (NCBI taxid: 1126212) database (http://blast.ncbi.nlm.nih.gov). Hits were filtered, and only high confidence peptide matches with a maximum protein and peptide false discovery rate of 1 % are shown.

2.5. Nematode Caenorhabditis elegans culture and toxicity test

The *Caenorhabditis elegans* var. Bristol (N2) strain was obtained from the Caenorhabditis Genetics Center (CGC) and kept as stock cultures on nematode growth medium agar plates (NGM) (17 g/L bacto agar, 3 g/L NaCl and 2.5 g/L bacto-peptone; supplemented after autoclaving with 1 mL of 1 M $CaCl_2$, 1 mL of 1 M $MgSO_4$, 25 mL of 1 M KH_2PO_4, and 1 mL of a solution containing 5 g/L cholesterol, prepared in ethanol) seeded with *Escherichia coli* OP50-1 strain at 20 °C as described by Brenner (1974). Gravid hermaphrodites were washed off the plates with M9 buffer (6 g/L Na_2HPO_4, 3 g/L KH_2PO_4, 5 g/L NaCl, 3 g/L $MgSO_4{\cdot}_7H2O$) and synchronized by exposure to a bleaching mixture (0.45 N NaOH, 2 % HOCl) following standard procedures (Stiernagle, 2006).

The toxicity assay was performed, with modifications, as described in Höss et al. (2011). For this test, 48-well polystyrene microtiter plates were used and 0.225 mL of the freshly prepared NPs solution in M9 buffer was mixed with 0.025 mL of a food medium (consisting of a suspension of freeze/thaw inactivated *E. coli* OP50-1 prepared in M9 buffer to reach a final optical density (OD) at 600 nm of 1 unit and cholesterol to achieve a final concentration of 0.1%). Ten age-synchronized L1-stage worms were transferred to each test well and four replicates were set up for each concentration. After 96 h of incubation at 20 °C, the test was stopped by heat-killing the worms at 50 °C. The samples were then mixed with 0.25 mL of a solution of rose Bengal (0.5 g/L), to stain the worms for easier counting, and stored at 4 °C until further use. The experiments were replicated three independent times.

Body length was measured at 40 × magnification using a light microscope. Images of individual nematodes were prepared (Nikon Eclipse 50i microscope) and the body length was measured along the body axis using ImageJ software (Schneider et al., 2012). Reproduction was quantified by counting the offspring of L1 larvae under a dissecting microscope at 25 × magnification and dividing the total number of offspring by the number of introduced tested organisms. Percentage of gravid organisms was calculated like the hermaphrodites with at least one egg inside their bodies of the total of nematodes tested.

In vivo toxicity studies with bio-AgNPs and AgNPs were reviewed using an analysis grid and assessed for quality using ToxRTool (Toxicological data Reliability assessment Tool, https://eurl-ecvam.jrc.ec.europa.eu/about-ecvam/archivepublications/toxrtool), a tool that ranks the studies according to the Klimisch criteria (Klimisch et al., 1997).

3. Statistical analysis

Experiments were performed in triplicates, and values are shown as the mean ± standard deviation, significant differences were determined according to Tukey's multiple range test. Prism 5.01 2007 (GraphPad Software Inc) software was used throughout the study to analyze all the data. For *C. elegans* toxicity test, data were presented as mean ± standard error and significant differences between means were determined with ANOVA following Dunnett's test to compare each NPs concentration with the control. Proteomic analyses were carried out with two biological replicates, each with three technical replicates.

4. Results

4.1. Synthesis and changes in the stability of bio-AgNPs in comparison with chemical AgNPs

Bio-AgNPs and chemical AgNPs were well dispersed in the aqueous solution, and synthesis was validated immediately by UV–visible absorption spectroscopy (Fig. 1A). We observed the typical broad peak at 420 nm for bio-AgNPs and at 414 nm for chemical NPs. We also detected the presence of a sharp peak at 250–280 nm only for the bio-AgNPs (Fig. 1A). After a period of 30 days of storing the NPs in absence of light under room temperature the stability of the SPR (Surface Plasmon Resonance) for both NPs was analyzed. SPR peaks for both NPs decreased in intensity, but to a different extent for each type of NPs. The SPR band of the chemical AgNPs was barely distinguishable (Fig. 1A), and the color of the suspension changed from an amber shade to opaque gray (data not shown). The SPR band for the bio-AgNPs was still observed in the UV–vis spectra although shifted to slightly higher wavelengths (Fig. 1A), and the color of the suspension did not suffer modifications (data not shown).

SEM analysis revealed that the bio-AgNPs obtained from *M. phaseolina* cell-free filtrate were spherical with an average size of 40 nm forming agglomerates (Fig. 1B). Chemical AgNPs were also spherical but more homogeneous in shape with a size of 20–30 nm and highly dispersed (Fig. 1B).

4.2. Antimicrobial activity of bio-AgNPs and chemical AgNPs

Fig. 2 shows the bactericidal activity of both bio-AgNPs and chemical AgNPs on *E. coli*. Bacterial growth kinetics were clearly suppressed after being subjected to the addition of different concentrations of both NPs. However, the detrimental effect of bio-AgNPs against *E. coli* was statistically different compared to chemical AgNPs ($p < 0.0001$). In this sense, the reduction in growth was 69 % when a dose of 5 μg/mL bio-AgNPs was added. Moreover, doses of 10, 20 and 50 μg/mL decreased bacterial growth by more than 86 % compared to the control treatment (Fig. 2A). For chemical NPs, the treatment of 5 μg/mL reduced the biomass by 82 %, and the doses of 10, 20 and 50 μg/mL showed the same effect as ATB and presented growth reductions in a range between 87.3 % and 91.8 % (Fig. 2C).

To accurately determine viability of cells after being exposed to the NPs, XTT reduction in microtiter plate assay was assessed 24h post treatments (Fig. 2B and D). Metabolic activity was undetectable under antibiotic treatment, in agreement with results observed for growth kinetics (Fig. 2A and B). *E. coli* respiratory metabolism responded to the AgNPs and bio-AgNPs treatments similarly. For bio-AgNPs, the metabolic activity was reduced 62 %, and 82 % for chemical AgNPs under treatment with 5 μg/mL (Fig. 2B and D).

4.3. Characterization of proteins associated to the biogenic AgNPs

Proteins decorating the outer layer of the bio-AgNPs were analyzed by SDS-PAGE electrophoresis (Fig. 3A). Proteins present in the *M. phaseolina* cell-free filtrate (CFF) were concentrated and used to compare against the bio-AgNPs exposed to reducing conditions (Fig. 3A). For both samples in comparison with the molecular weight marker (MW) several bands ranging in between 170 and 25 kDa could be

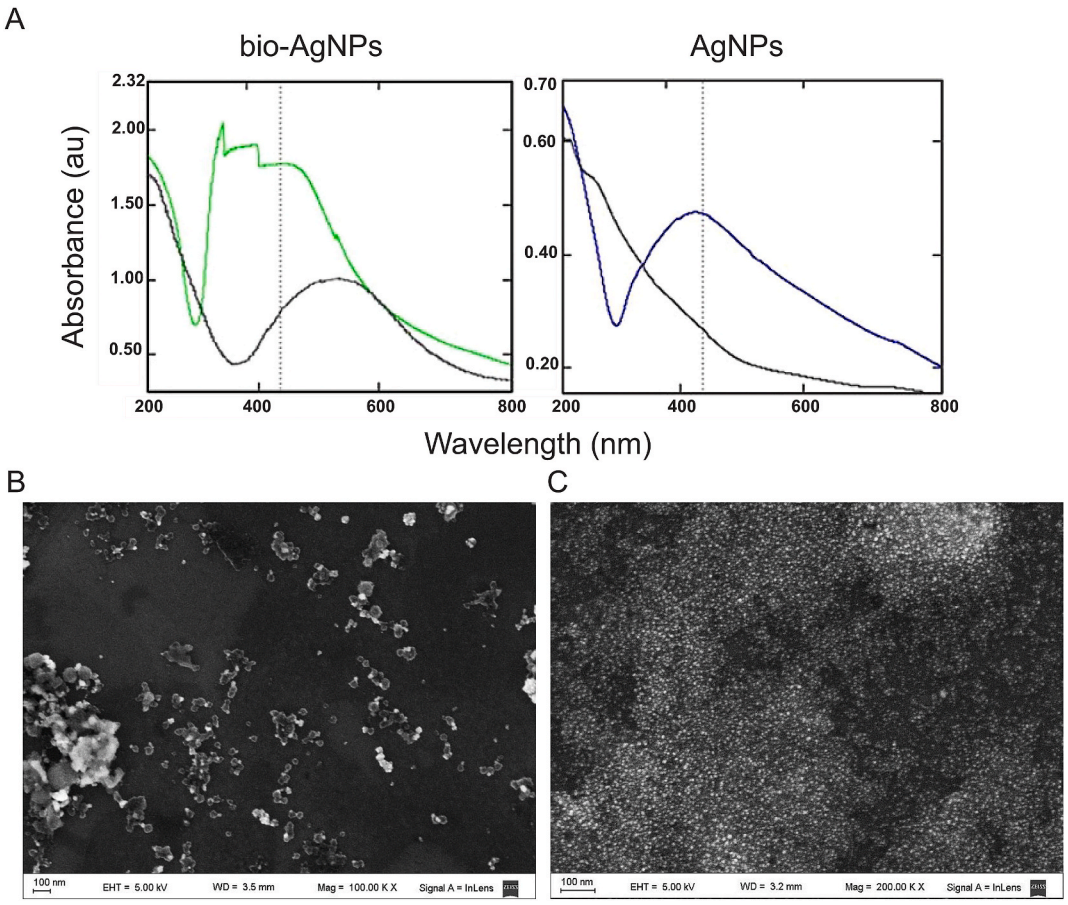

Fig. 1. Kinetics of synthesis and stability of bio-AgNPs in comparison with AgNPs. A) UV–vis spectra recorded for the biogenic and chemical NPs after synthesis. Changes in the stability for both nanoparticle solutions after 30 days are shown in gray. B) Scanning electron microscopy (SEM) micrograph of nanoparticles (bar = 100 μm).

observed (Fig. 3A). Only exposing the bio-AgNPs to both reducing conditions and high temperature resulted in detachment of the capping proteins from the NPs (Supple. Fig. 1). Zymograms conducted in Native PAGE gels under non reducing conditions revealed the presence of only one major band (approximately 50 kDa) that developed strong color for both the CFF and proteins coming from NPs with strong oxidase activity using guaiacol as substrate (Fig. 3B).

4.4. Proteomic analysis of the components of the bio-AgNPs

To depict the constituents forming the corona in the bio-AgNPs, we based the analysis on the presence of the same peptides in all the independent biological replicates evaluated by LC-ESI/MS (Orbitrap). We detected 59 hits for the fungal cell-free filtrate and 46 hits for the bio-AgNPs. The proteins identified corresponding to both samples were classified according to their function registered in the Uniprot database (Fig. 4). Most relevant hits for bio-AgNPs are shown in Table 1. Following these criteria, our proteomic data revealed that 60 % of *M. phaseolina* proteins forming the corona in the bio-AgNPs are hydrolytic enzymes (Fig. 4 and Table 1). Also 21 % of the proteins detected were related to oxidoreductases and a 2 % to carbohydrate binding proteins. In addition, from hydrolases, 96 % corresponded to glycosidases and 4 % to proteases. While proteins detected in the CFF showed 53 % that corresponded to hydrolytic enzymes, 18 % to hits related to protein synthesis, 5 % to virulence factors, 3 % to oxidoreductases, 3 % to carbohydrate binding and a 3 % to nucleic acid binding proteins. Analyzing the hydrolases from the CFF we identified an 82 % linked to glycosidases, 15 % to proteases and 3 % to lipases (Fig. 4).

Amongst the most relevant hits associated with the bio-AgNPs corona, we identify hydrolases, several of them amylases, a chitinase, peptidases and phosphatases, all of them carrying signal peptides (Table 1). Also, enzymes involved in catalyzing oxide-reduction processes, like a glucose-methanol-choline oxidoreductase, FAD linked oxidase, peroxidase and a multicopper oxidase were identified (Table 1).

4.5. Effect of bio-AgNPs and AgNPs exposure on growth, reproduction and fertility in C. elegans

To evaluate the effect on growth, reproduction and development of *C. elegans* caused by exposure to bio-AgNPs compared to chemical AgNP, body length, offspring and fertility of nematodes treated from L1 larvae to adult stage with different concentrations of NPs were measured (Fig. 5). Nematodes exposed to the M9 buffer without any NP were assayed as a control group. The average body length of *C. elegans* in the control group was 1254 ± 28 μm (Fig. 5A). Notably, nematode growth did not significantly change with any of the tested bio-AgNPs concentrations in comparison with the control group (white bars in Fig. 5A). Furthermore, for chemical AgNPs, no difference in *C. elegans* body length was observed under concentrations ranging the 0.001–10 mg/L (gray bars in Fig. 5A). The body length of worms treated only with chemical AgNPs at 100 mg/L was significantly decreased (Fig. 5A, $p < 0.0001$).

Results of counting the offspring per treated organism with bio-AgNPs did not show significant differences compared to the control group in concentrations from 0.001 to 1 mg/L (white bars in Fig. 5B). However, treating the nematodes with 10 mg/L of bio-AgNPs reduced the size of the offspring by 15 % ($p < 0.05$), while 100 mg/L did it by 99 % ($p < 0.0001$) in relation to the control group (white bars in Fig. 5B).

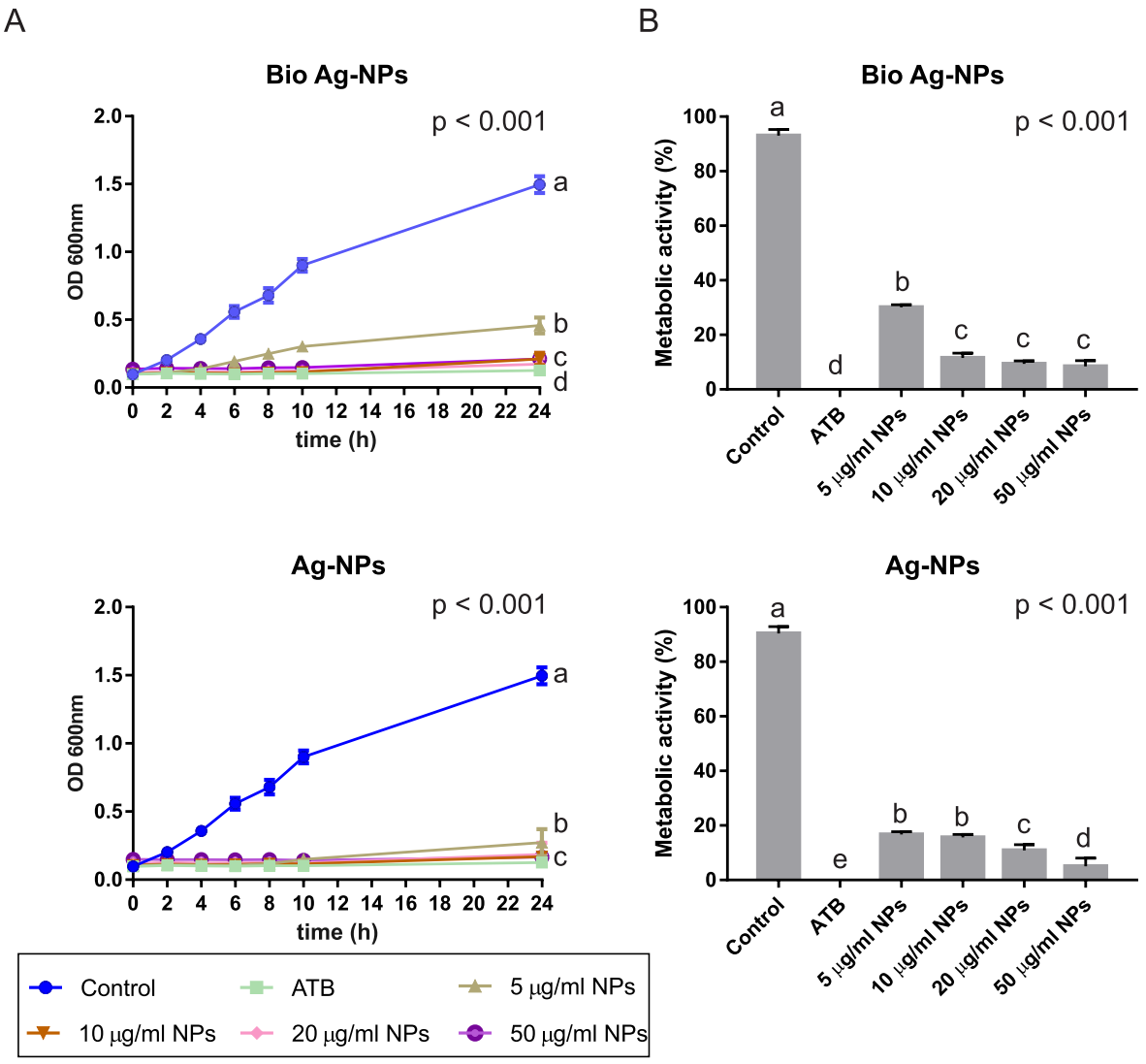

Fig. 2. Bactericidal activity of bio-AgNPs vs AgNPs. *E. coli* was used in microtiter plate assays to monitor A) growth and B) metabolic activity after being subjected to different concentrations of bio and chemical NPs (5, 10, 20 and 50 μg/mL) up to 24 h. Control corresponds to bacterial cells in absence of NPs. ATB, ampicillin (100 μg/mL) was included as a positive control. Metabolic activity at 24 h time point was detected by XTT reduction assay. Values are the means of three different experiments, and bars indicate SD, different letters indicate significant differences ($p < 0.05$), according to Tukey's multiple range test.

Comparatively, nematodes treated with 1, 10 and 100 mg/L of chemical AgNPs showed a significant decrease in the reproduction by 20 % ($p < 0.01$), 99 % and 100 % ($p < 0.0001$) respectively, (gray bars in Fig. 5B).

Regarding fertility, no significant differences were found in the percentage of treated nematodes that reached sexual adulthood under any of the concentrations of bio-AgNPs tested compared to the control group (white bars in Fig. 5C). Likewise, the treatment with chemical AgNPs during nematode development did not significantly affect the percentage of gravid adults at concentrations of 0.001–10 mg/L (gray bars in Fig. 5C). Nevertheless, the group of worms treated with 100 mg/L of the chemical AgNPs showed a complete inhibition of the sexual maturation since none of the nematodes in the treated group reached the gravid stage (gray bars in Fig. 5C ($p < 0.0001$) and Fig. 6). It is important to highlight from the assessment of the toxic effect of NPs treatment during the *C. elegans* development on growth, reproduction and fertility, that the three variables were affected by chemical AgNPs in lower concentrations than those of bio-AgNPs.

5. Discussion

In the nanotechnology field, research has progressively redirected its focus to the production of NPs and nanomaterials using living organisms or the byproducts of their metabolism to achieve desired features in green synthesized particles. Different bacteria, fungi and plant extracts were described to use oxidoreductive molecules to synthesize NPs intra- or extracellularly (Singh et al., 2016; Khan et al., 2017; Mohamed et al., 2019; Erdogan et al., 2019; Ruttkay-Nedecky et al., 2019; Spagnoletti et al., 2019). However, fewer are the papers that reported the molecular identity and possible role of the enzymes that act as precursors in NPs biosynthesis and further capping process (Barwal et al., 2011; Ballottin et al., 2016; Quinteros et al., 2019). Herein, we provide a series of results that show biogenic AgNPs to be comparable with chemical AgNPs at biocidal activity but prove to be less toxic in the nematode model *C. elegans*. We also describe the composition of the protein corona on bio-AgNPs and suggest that these fungal secreted molecules are involved in the green synthesis process, as well as in modulating the particle

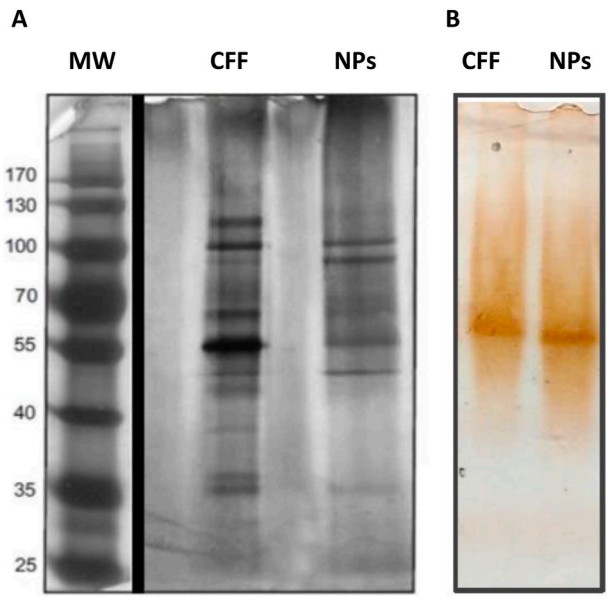

Fig. 3. Analysis of capping protein decorating the biogenic AgNPs. A) Comparison of protein profile by silver staining of 10 % SDS-PAGE. MW, molecular weight marker; CFF, proteins present in the aqueous cell-free filtrate from *M. phaseolina*; NPs, bio-AgNPs. Samples (25 μg) were loaded after heating at 100 °C for 10 min under reducing conditions with 1 % SDS loading buffer. The black space shows the separation of two independent gels. One of three independent experiments is shown. B) Zymogram to detect lacasse activity in the samples using guaiacol as substrate. One of three independent experiments is shown.

stability by capping the metallic core.

Though production of NPs using biomolecules has recently gained interest due to their non-toxic nature and not involving harsh synthetic procedures, from the perspective of green chemistry, there is still a drawback in biological synthesis versus conventional chemical one, this being NPs size heterogeneity. However, some of the many advantages of biogenic synthesis allow efficient surface functionalization and stabilization of particles, biological compatibility with lower toxicity, and unique optical features (Huang et al., 2015; Schröfel et al., 2014).

For this work we synthesized chemical AgNPs using sodium borohydride, and bio-AgNPs starting from an aqueous cell-free filtrate from the fungus *M. phaseolina* as we previously described in Spagnoletti et al. (2019). Both syntheses rendered spherical NPs with a SPR corresponding to silver at 414 for chemical and 420 nm for bio-AgNPs (Fig. 1). We detected another band in between 250 and 280 nm only for the bio-AgNPs (Fig. 1). An absorbance peak at 280 nm arises due to electronic excitations in the aromatic amino acids tyrosine and tryptophan (Toledo et al., 2013). Thus, this band indicates the existence of proteins attached to the NP secreted by the fungus in the cell-free filtrate.

Furthermore, after a period of 30 days, we analyzed the stability in suspension for both NPs, finding that not only the SPR peak had changed but also that the color of the chemical AgNPs solution had shifted to opaque gray color, while the bio-AgNPs retained most of the original color and shape of the SPR peak at UV–vis spectra (Fig. 1). These results strongly suggested the presence of a capping agent in the bio-AgNPs protecting the particles from aggregation.

Even though the bio-AgNPs presented a corona, absent in the chemical NPs, and that this extra layer of macromolecules could have been an obstacle in the interaction with cells, the bactericidal activity against *E. coli* was found not to be compromised (Fig. 2). For chemical NPs, exposure of bacteria to a dose of 5 μg/mL reduced growth by 82 %, and 69 % for bio-AgNPs. *E. coli* respiratory metabolism responded to the AgNPs and bio-AgNPs treatments similarly (Fig. 2). Therefore,

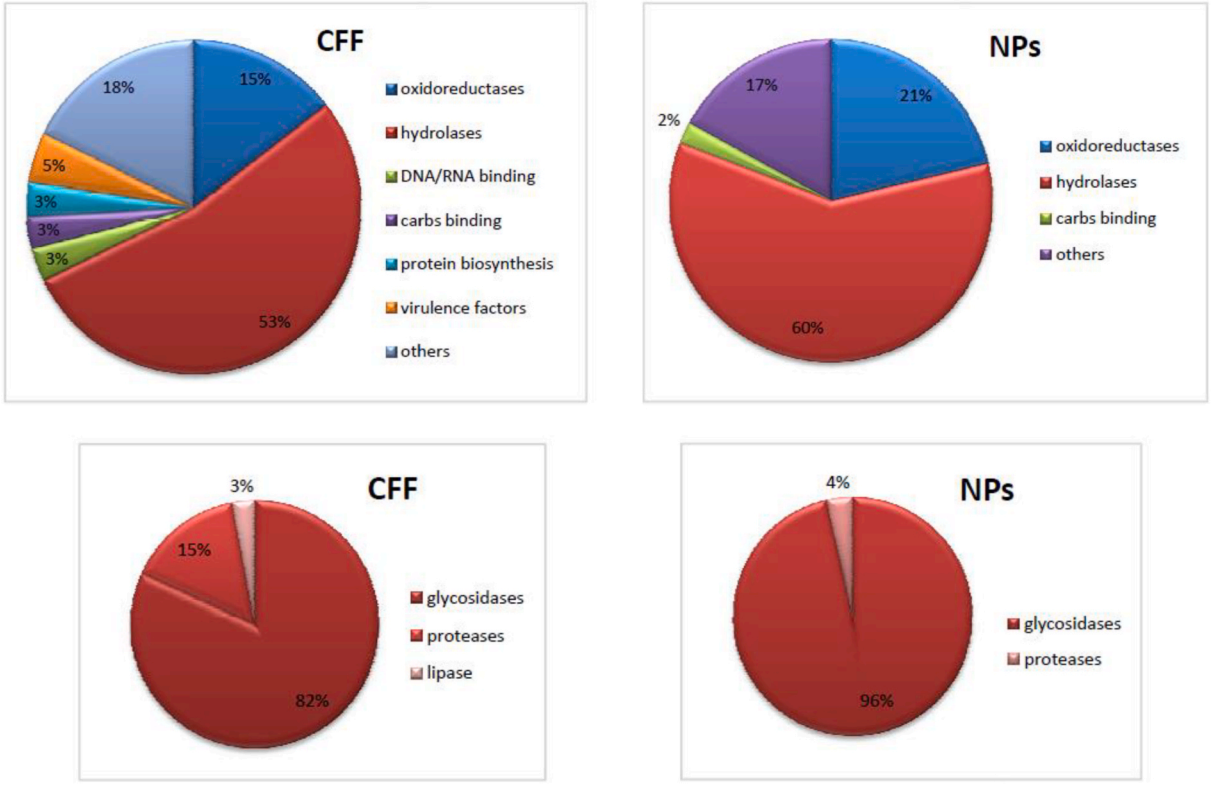

Fig. 4. Proteomic identification of corona components in bio-AgNPs. Functional annotation and relative abundance of proteins identified in bio-AgNPs (NPs) and in the aqueous cell-free filtrate from *M. phaseolina* (CFF).

Table 1
Most relevant proteins associated to the bio-AgNPs identified by Nano LC-ESI/MS.

Protein Name	Accession number	MW	Coverage (%)	Peptides	Protein sequence (matching peptides are shown bold and underlined)
Alpha-amylase a type-1	K2QLM3	54.6	19.3	TEDSAVQSGYETWIR; SGCKDTTLLGTFSENHDITR; KGFDGFQLITVLSNK; EAVWLSGYNTNADLYR; FAALTSDLSQAK; ALAAELHDR; SIYQVLTDR	MKTSLLSAAIAAAICGTASAATPAQWRSR**SIYQVLTDR**FARTDGSTTAACNTQDRQYCGGTYQGIINKLDYIQNMGFTAIWISPVVKNLPEDTGYGEAYHG YWQQDLYSLNTNFGSVDDLK**ALAAELHDR**GMYLMVDVVVNHNGWAGSAGSVDYSRFHPFNSQQYYHSYCEVSDYSNQDLVEDCWLGDSTV ELVDLK**TEDSAVQSGYETWIR**QLVANYSIDGLRIDTAKHVDKAFYPGFLDAAGVFATGEVFDGNPSYTCDYQNYMDSVLNYPVYYPLVRAFTSPSGSISD LVNMINTLK**SGCKDTTLLGTFSENHDITRFAALTSDLSQAK**NVIAFNILSDGIPIIYEGQEQHFAGAEDPDNR**EAVWLSGYNTNADLYR**FTASVNQIRNQA IAKDANYLTYKNWVIYSDTTTIAMR**KGFDGFQLITVLSNK**GARGDAYTLNLGNTGWTSGTRVVEILTCSTVTVTSSNTVTVPMANGLPRIYFAASNLS GSGICNL
Glucoamylase	K2S7L9	67.8	12.4	ATSMIAYAH WLINNGYSDTAR; VAGAAAGIVVASPSK; SIYNINSGIAQGR; LQGVSNPSGDLR; SYTVPSGVA TATISDTWR	MLFPSKALALVGLLVGDALAIPATTLRKRQSSVDTFISTESPIAYAGVLANIGDDGSK**VAGAAAGIVVASPSK**SNPDYFYTWTRDASLVFKALVDHFIAGDY SLQDEIEDFIISQAK**LQGVSNPSGDLR**SGAGLGEPKFNVDLTQFTGAWGRPQRDGPALR**ATSMIAYAHWLINNGYSDTAR**DVVWPVIRNDLSYV SQYWNQTGFDLWEEVQGSSFFTIAVSHRALVEGSTLASALGQSCSYCDSQAPQTLCFLQSFWTSNGNYVVSNINTNNGRTGKDANSILASIHTFDPDAGCD DSTFQPCSARALANHKAVTDSFR**SIYNINSGIAQGR**AVAVGRYAEDVYYNGNPWYLTTLAAAEQLYDALYTWTREGTITITSVSLPFFRDIYSSA AVGTYASGSAAYTSILNAVKTYADGYVSVVQKYTPSSGALAEQYSRNDGSPLSAADLTWSYAAFLTAIARRNSIVPASWGGETANVVPGSCVATSA IGTYASATNTVFPTSQTSNPGATTTRPPTSSTTTTRVTSSTTTTTTNPTSVAVTFNVIATTVFGENIFLAGSIAALGSWAPASAKALSADKYTSSNNL WYVTVSLAPGTSFQYKYIRKSSSGAYTWESDPNR**SYTVPSGVATATISDTWR**
Phosphoesterase	K2RUW5	43.9	9.6	VLAILLGDAVPER; SYVKPNVDAEYAG; TFLEPLLDNPK	MARFTTSLLALLALGDAAVALPGKLQRRASEVPTLSPTTFVKGKAFDRIAIIWLENTDYDKAEGDPNLAWLATKGIKLNNYHAVTHPSQPNYLAAIGGD YFGMNNDDLSTFDGNISSIIDLLEDRGISWGEYQEDMPYTGYTGKAYPNPATGANMYVRKHNPAVSYGNVLDKPERLGVTKNLTLFQQDLENETL PQWMFITPNMTSDGHDTSVTVAGTWTR**TFLEPLLDNPK**FMNNTLVLVTFDENETYTIQNR**VLAILLGDAVPER**LVGTTDSTFYDHYSEISTVQANWCLDTL GRFDVGANVFSLVADKTGDTLREWSGPQALEQRYFNYSYAGVFNERSGAAR**SYVKPNVDAEYAGR**KVHPSVVDTWKDSDLPSYYTTDL EIPDGLNPPEGY
Six-hairpin glycosidase-like protein	K2RAI2	76.7	6.9	ELSLDLVPQEIY DQQSAFYPTVESR; TQNLDWLNQHY DILR; FGVPLDTR	MLPLYLLAACFTGFVSAQAQSTFSPARPPALPLAVKSPYLNTWLNAGSDGGNGGYLAGQWPVHWSNQITGWAGLIRVDGTTYKWLGDPLGPGGPAVVTQN SFEYTSTKSLFNQNVEGKVALNITFLSPVTPDDFRRQSLVFSYLNVEVASIDGAEHDVQLYSDISAEWVTGDRSRTAQWEYDTSDGIAYHKVYRQTQQIFSE NADQAEWGNWYYATDAADGVTFQSGADNDVRAAFQSNGSLANTKDTNFRAVNDRYPVMGFAKDLGSVGSAAVSTLFTIGLAQQDAIQFAGSDGYLPRPS LWTDYFSDDIAALSFFHKDYSTSEEKSTALDNQISGDAIGAAGQDFLTITSLSVRQVFASIQLVGTQDKHWIFLKEISSNGNMNTVDVIFPAHPLFLYTNPELLR LVLEPLYENQESGQYPNDYAMHDLGSRYPNATGHPDGLDEPMPLEECGNMLIMALAYYQR**TQNLDWLNQHYDILR**RWTTFLVDEALYPNNQLSTDDFAGTL ANQTNLALKGIIGIEAMSKIAELTGNTTEASTDHDTATSYISQWQKLAVVPESGGTPAHTNLAYGDADSHGLLYNLFADR**ELSLDLVPQEIYDQQSAFYPT VESRFGVPLDTR**NTYTKTDWEMFVAAIASTETRDMFHSDIADWISQTPTNRAFTDLYETETGDYPSGITFVARPVMGGTFALLLLQM
Six-bladed beta-propeller TolB-like protein	K2RHJ5	47.7	11.6	FRPSTGEVVVVDS TLQHPNGIAFS R; RNIFQSL EGSPDGIK; NIFQSLEGS PDGIK; TLYLVG IGGITK	MPASLLSLAALLSVGGSARAAATGFSQLSNSSAPAANSGYAPVAAPCGPSTANVTCIHRYGSVLPPSFSRDPDPNVGYTGTLVPDDPSWASLVPTADFVIFD KERGLSMLGATPRIWHNYIPVLNVIHEAPIFVPELNKLFTTQDGPPGNLSNIVIDLNADPPTVEAFVTDPPVYQPTGGILHDGMIYWAVQGNNVSLPNGLQ QRPGIVRVDPRTYKAEWLLNNYYGFFYGGLNDLTVDSVGDVWFTDSDYAWGLGLSNQSNQNQLATYR**FRPSTGEVVVVDSTLQHPNGIAFSR**DGATL YVTDSGLETVGAPGTETDAGFYNYPIRIEFTSTNARNIYAWDIARPDGPKGTPVITGK**RNIFQSLEGSPDGIK**VAANGYLVVGSGLSNGVDVLDARGSPIAR IQTNHPVENIAFAGDDLK**TLYLVGIGGITK**VEWDLQGPDPNNYYL
Carbohydrate-binding	K2S399	99	5.6	WEYVGCLLDSPLAR; MYHSEATLMDDGR; LSIWSNADLK; D VSFTGGAGA GACYLK	MNAPLNWARSSAQLLLLFASFSPLLADARYVNINDKRQEATPTSTAVSTAAPACPASDGVTYQLASGSTFLIECSVDRVANDLKTVDPVANFAACIQAC DTTVNCK**DVSFTGGAGAGACYLK**SAAGTISTNTGVWGAKLVAKGSAASSSAAASSTAPPAGGGSATTSPVASSTDTRPPSASVPAGWELKGCYVDSVNA RSMNNLQPDDADQTVESCVNTCIGLGHTVAGMEYGVQCFCDDFLRNGAEEAAAGDCSMSCPGDASQTCGAGNR**LSIWSNADLK**VYEPPAAQNTSLP GK**WEYVGCLLDSPLAR**VFQYEIVLENNNTAENCLTQCSNYGFDRGGMEYGNQCFCGDQADVDAAGATLQAESDCNMACSGNATYICGAGNRISYYQW SPEDPLYVWHYPKGADAGSYELLIGGVVIPLVSIPARNGKIAFVEKFGTGPPNSTGAYELDPSLINDFSAAWRTMHVKTDVFCSGGVTLPDRAGRILNVGGW SADSLYGVRLYWPDGTLGTAGTNDWEENYQELALQAGRWYPSAMVMANGSVLVVGGMDGSNGNAVPNMEVVPRPAGGQLVYADYLLRTHPYSTYPF LAVLPSGGIFISYYNEARILDENSLQTIQTLPNIPGAVNRPDGGRTYPFEGTAVLFPQHAPYTDPVRVLICGGSAPGQPPALDNCVHMTPDAPEDGWTIER MPSKRVISCMTALPDGTYLILNGAFRGEAGFGLATGPNLNAVLYDPAKPLHQRFSVMANTTVAR**MYHSEATLMDDGR**VIVSGSDPQDARYPQEYRVEVF TPPYILSGAPRPSFTLSSDDWAYGAQASFTVSGATTGNVRVSLMGSVVSTHGNSMGQRTIFPDVSCSGTTCTVTAPPNKYICPPGWFQMFVLDGPTPSHAQ WVRIGGDPAELGNWPPYDDFTTPGLGATLPLTGAAATSQSRLASNVSRMG
Peroxidase	K2SCI0	32.9	9.9	GFSEIDLVALVGAHSTAK; SSASVLIDQFAAK	MLFSKSSIFLLSTAASVQALSLSDVSSAASVLKREASGLGNNLLSLVHRRDSCPDVWQKVASELKGWFLDGSVCSDDARAAIRLSFHDCFSGGCDGSIILAHE YTRSDNAGLADFAMKLAPLADQYEVGTADLIQFAGALATATCPLGPRIAVKVGRQDSSTPSAEGQLPSSR**SSASVLIDQFAAKGFSEIDLVALVGAHSTAK** QFFDQPDKAGQSLDSTPGTWDTNFYRQTTLGTAPVTLESDKNLATDLRTAVQWTAFNAQGVWAAAYVSAMNKMTVLGNDVSSLTDCTSVISAATSKRDKAAPIADRI
Chitinase	K2QYV1	44	8.6	TMVSYDTV GSAK; AALDSYANT FAAK; MVLG MPLYGR	MGGGTGYRSVVYFVNWAIYGRNHNPQDLPLNQLTHVLYSFANVRPETGEVYLTDSWADTDKHYPTDSWNDVGTNVYGCVKQLYLLKKKNRNFKTLLS IGGWTYSSNFAPAAATAAGRANFASTAVQLVKDLGFDGLDIDWEYPADDTQAQNFVALLAATR**AALDSYANTFAAK**NLTRPTFLLTIAAPAG PTNYQKLRLAEMEPYLDFVNL MAYDYAGSWDTKAGHQANLYNSTSNPDSTPFNTDQAMKYYTANGIPSAK**MVLGMPLYGR**AFQNTDGPGKAYSGVGAGSWENGIWDYKALPRPGA TEYYDAEAGASYSYDGSSR**TMVSYDTVGSAK**TKVGYIQAKALGGAMWWESSGDKSGTDQSIISNVWTSMAGADGGMAEQSQNNLNYPDSKYDNLKAGMPGQ
Glycoside hydrolase	K2RZ42	40.6	7.9	AGELNLPER; DYMVGLSAL QYK; NAYNTNLYR;	MTCHFGLRSALAAVTSSVLYCTHLAAAKAVFAHYMVGTTTDAHAATDITTAAAAGLDGFVLNIGDPRQSYVTNTVSSLFSHAPSTPSFTLLFSLDLAAGLGA GASLADYDALLKKYTAHASYARGGAHGYPFVSTFSDGGLSNETWDEWRGRVFGNEVYFVPDFDQTQGYYDAATGWWDHWGGVLDGLFSWEAAWPER NGYGGAFPGDVGPDVDVAKGAASRGK**DYMVGLSALQYKNAYNTNLYRAGELNLPER**MKNVLEMTPAPEYAEFITWNDGPESHYIGSLWPEQNTDA DPARYATQTLAPHTGWLPLISSFAAAFRANASSASAMRPAPATDAATGALWYKAILQSASCPNEGNGGVYAKPDGWAKGEDVLSWAVV

(*continued on next page*)

Table 1 (*continued*)

Protein Name	Accession number	MW	Coverage (%)	Peptides	Protein sequence (matching peptides are shown bold and underlined)
Histidine phosphatase superfamily clade-2	K2S9T6	71	4.4	AVGIGYVQE VLAR; LDIEVIQAP HPVLPQR	MFQGEQANLGSAADRDVRYRPKCWEDSTVQKLTLAHVPSHSGPFPAPLASSFRFPCASDVQSETAPRGEKLQKTPRSRQKSETASRRNLVRADLNQAM FGRVFTIAAAAAGLCAEAAVVELRDAAATTASASTTVPQYFQTSPELYAGPTATGKAPFLAETNIAPFSGVSYIAPQPLETQQPILGNTKNANIFQQMGQL SPYFANPDGFGVHEHPLPAGANITQVHVLHRHGARYPTSSDGSIALAQKIVNATGTFNATGDLAFLNGWTNKLGAEILVPVGKQQLFDSGVSHYYNY GHLYPNNGSKIIARSTTQDRMTQSAEYFLAGFFALQWPQNASLELIIEQQNYNNTLAGYYQCNNSNAAVNKGGSNATLEWASTYLVNATSRIASQV PGLNWTASDSYYAQSLCAYETVALGFSHFCSLFTYAEWLGYEYSIDLSFAGGYGFQSPTGR**AVGIGYVQEVLAR**LNHHLIDTPTAQVNVTLDNSTATFPL DQQLNFDFSHDTNIMSILTAFGLKQFAPFLPPTQYTANRSLIVSHMEPFAAR**LDIEVIQAPHPVLPQR**GGSEAYNTAAGATKYIHFILNQRTVPLHASFPE CEARDDGWCELETFMKVQATKLEEAQYDWACWGDYGAVPYGTITDGVPVATPTGTFAAEL
Glycoside hydrolase	K2RH66	46.4	7.5	VLIDLHGAPGSQNGYDNSGQR; IADAGFNLVR	MLSRYFASALLATTVVFGAAIEKRKVSFNWGGEKVCGLNIGGWLVLEPWITPSIFEQFDASQGIIDEFTLNEKLGRDKALEVLKPHWDSWVGFEDFQR **IADAGFNLVR**IPVGFWAYDTFGSAYSQGAAPYIDAAIDWARGTGLK**VLIDLHGAPGSQNGYDNSGQR**METPQWLQGDTVNQTLSVIQQIADKYAK TEYQDVIAGIQLLNEPAGYELDVNAIKQFDRDGYAKVRSVSDTTVVIHDAFQNPSSYNGWMTPSDNNVQNVVLDHHEYQVFDNGMIKWSAAEHRQ GVCNNRARWEGSDKWTIVGEWTGAMTDCAKWLNGYGRGARYDNTFEGAGYVGDCGFASDLDSWDQQRKDDTRWYIETQLSAFEKIDGWIFWN FKTEQAPEWDWGKLSAAGVFPNPVTDRKFSAVC
Glucose-methanol-choline oxidoreductase	K2S169	68	4.6	TDAMLEMEP HESLPGAS; AQD DAALDDVIR	MCLWDFAFILTLVIGVQAKLGRLAQVVGRDVSLQDSYDFVVAGGGTSGLTVADRLTEDPNITVLVIEYGPLDKHEDSVLVPGLLDLDTTPYWFNLTSAP QEGLNNKTFRVPAAAVVGGGTVINGMFFDRGTAADYDLWEQLGNPGWGWDGLLPYFRKSENFTPPAESFAAEWNISWDLSAHGREGPVQSSFPVFQF GSTKNFLRACLSLGLAKPSDQASGNKAGVSWVPSSLDYTNQTRSYSRVAHYDRVISSRPNYHLLTMHTVSKVLFSDDNAATGVEYFSRETGEVSTVTA SKEVIIAAGAVHTPQILQLSGIGPKALLDSLDIPVVKDLSGVGHNLQDHPAIYTQWNFSNLPLPSVESLDVNQTQIDEALFLYRTNRTGAFTQVDRGGNQ AAFVPLSKLLSSSPSTYASILALAASTSPTDIYPPSTPPSVLAGYIQQLARIIPQLSSPTEPVYEFTSGGSSTLPVVFLKSLSRGTVAITSTNASTQPRVDYRTI RAPSDIAVVRAALRWARTLMR**TDAMLEMEPHESLPGASAQDDAALDDVIR**ANANPGYQHVTASCAMMPEEWGGVVDSRLRVYGVERVRIVDASI MPVIPGTHTSSTVYAVAEKAADIVKKDHGITIGMLKGH
Amido-hydrolase 2	K2QWP0	36.2	7.8	HSIVAISSPGSGV YPGDEASA VGLAR	MRSLAWKFASAALFGVALSTILETQRDNIGRRSTTVDVEVIIQDAAADGINLTALPFSAAALASIQAISIPENMTLSEPGNSSRVDVHVHAVPDWYRELVPIT GQNPTPAWDIQTHLAFMANNSIK**HSIVAISSPGSGVYPGDEASAVGLAR**LLNEWMAALCRTYPDRFSFYAVIPLPYTTAAIAEANYALSKLGAVGVIVL SNHEGKYLGNQQFKFAALNSRNDSREIVYIHPNEPVLNTNGTIVSANPTLYSSGFVEFYFETARTIMDLTLTQTIHNFTNIHYDYPYARATYEGSIEAIVT ADFVSASEKAGIFYGNARTLFASKIASL
FAD linked oxidase	K2S0X9	54.6	3.5	AVDAGAGD LLAFDDAADR	MTSLMRSVAAAALFGLAAVASADSLTCSTLESTSNISIDRRFELDYTTENSEYWSTGCAALKPACIIKPSNVQEMSTVIKTLYNNNETFAVK SGGHNPNQNFSSIDGGPLISTADLNEVTLDKASQTVRVGPGNRWEDVHKVLDGTGYTVVGGRIGNVGVGGYIIG GGLSFLSAEYGWAANNVVEFELVLANGTITTATNTTNASLFKALKGGGANFGVVTAYTLAAHPIGQVWGGNLIFGADKSSALLAALQNFTQN YPDEKAGIILTSEITGANLVHIWIMFLFYDGPTPPAGVFDMFTSL KPSTNNAKTRSYYDLLSYNNWAVLKGSAYTIATETTPLLPADSPQAVNTTVAHLQACYDHWVAVAKARAAVPGLVASIAFQPYPAAFARRAR**AVDAGAGD** **LLAFDDAADR**IIFEFDFSYLRGLDSVDVAVDEATVELYAGMKEIVDQAVDEGRAPDVYRPLFMNDGYWRQDYWGRISAESRAFAEGVRDEVDPGRFW SERSAGGFFL
Multicopper oxidase type-1	K2RRF6	60.5	2.4	YDVIITGLENPER	MIRLSLVLGFMATTLAKTVTLNWDIGWVSAAPDGFTRPVIGINGEWPPPVLEADVNDTIIVITRNLLRNETTSLHWHGMWHYNSTHMDGGARISQCEIPP GGTFTYKFKAYPAGTFWYHSHDMGQYPDGLRAPMIIHDPKAAAERDTDKEYVLTVSDWYRDQMPSLIHRYLTTSTYNSTMPNPNSSLINDQQSTTLNIR PGQKIYVRIINMSALATYYLQFDQHHLTVIAIDGVDVDPQTWEALEIIPGQR**YDVIITGLENPER**NYAFINKMATLGFQNNNVLSYDSSWPVPEPLNVGSF NLRSDFNLTPLDEELLLEPV DHTFTMEVNNVNVDGVGSRITQGPDPYIAPRTPTLYTTLSTGSNAINPAIYGQANAYVVEAGDIVQLVVNSNEPVTTNTSGRGHPMHLHGHTFQVVGQY GSPWDGDASKFPAVPMKRDTTVLFTGGSLVIRFRADNPGVWMFHCHNEWHLDAGMAGTIIEAPLELQQSGLTIPPQHLASCRALNLTTRGNCAGNTA NLEDTAACRVYDTEPWGALIKRDEETAY
Glycoside hydrolase family 17	K2STT8	32	5.8	AIDETQNFI NQYNPAAK	MKFTSAAVLLAGSAPMASALRKGFNIGATNADGSCKTQAQWAQDFKGMKNLPGNFKDVRVYAASDCNTLDLAVPAAKDAGIQLLVGIWTEDDAHYSAEK AALEAAITKYGVDWISAVSVGSEDLYRGDTTSWRLAEQVYDVRGMISQDKYGGKGIWVGHVDTYNAFNASSADLIQAVDFLGVDAYPYWQGVTPDQA QATFQK**AIDETQNFINQYNPAAK**LWITETGWPTAGPNFGNSVANKENAKTFWDAVLCKYASQYSIWWYTLHDTSTEAQDFGVVDDNFGALFDLNCPSS
Alpha-1,2-Mannosidase	K2RXQ2	56.7	3.1	LSDLLGD DEYAQLSQK	MALLSTPLLLLPALILLGATAAPHQPRQYSSTGGPNQTRADAVKEAFDFAWNGYYTYAFPNDELHPISNGFGNTRNNWGASAVDALSTALVMQNREIVN QILEYIPTIDYTTTSTEVSLFETTIRYLGGMISAYDLLKGPLSHLADNSTQVDALLEQSKVLADALKYAFDTPSGVPANNLWFTNNSDDGTPTNGLATVGTLVL EWTR**LSDLLGDDEYAQLSQK**AESYLLNPQPAYNEPWPGLVGTDISIENGSFVDASGGWVGGADSFYEYLIKMWVYDSDRFSEYKDRWILAVDSSIQYLAS HPSSRPDLTYLAAYDNQTTLNVSQHLACFDGGNFILGGNVLGRQDYVDFGLELVEGCRNTYVSTLTGIGPEIFSWNTSTLPGNQSAFYDKNGFWIRDGFYD LRPEVLESYYYAYRQTRDPKYQEWAWEGFVNINATSRQGSGFTAVTNVNAPNGGSPDDNQESFLFAEVMKYAYLIHAEEADYQVFGGDGGSNGWVYN TEAHPFKIAGSPI
Aspartic-type endopeptidase	K2R5R4	41.1	4.2	WYSVYDLGNDAVGIAK	MKLKKVPLAEQLEHANIGDHVKALSQKYMGSRPQLNSVEEIFKTQPIQADSEHPVPVTNFLNAQYFSEVSLGTPPQTFKVILDTGSSNLWVPSSECGSIA CYLHTKYDSSASSTYSKNGSTFEIRYGSGSLSGFVSNDVFTIGDLTVKDQDFAEATSEPGLAFAFGRFDGILGLGYDTISVNHIVPPFYNMIDQGLLDEP VFAFYLSDTNDEGSESVATFGGIDESHYTGKLTKIPLRRKAYWEVDLDSITFGDATAELDNTGAILDTGTSLIALPSTLAELLNKEIGAKKSFNGQY TVDCDKRDGLPDLTFTLTGHNFTITSYDYILEVQGSCISAFMGMDFPEPAGPLAILGDAFLRK**WYSVYDLGNDAVGIAK**AK

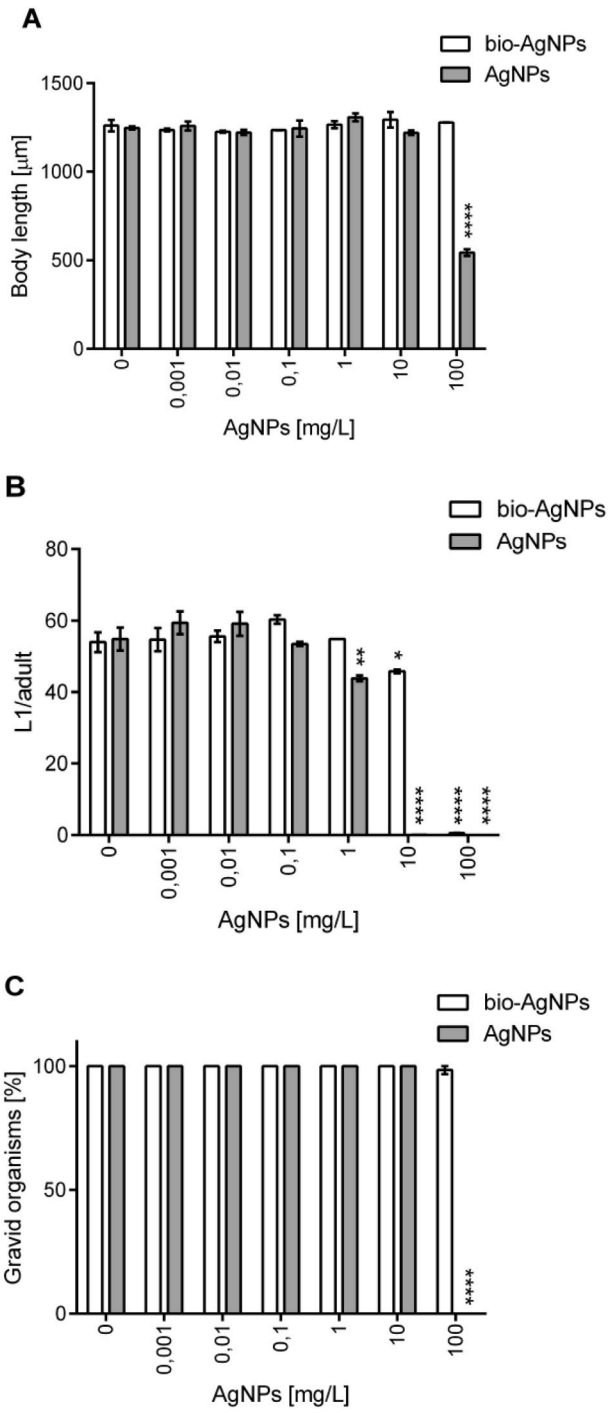

Fig. 5. Bio-AgNPs and AgNPs toxicity on *C. elegans*. A) Body length, B) reproduction and C) gravid organism showed as percentage of nematodes exposed to different concentrations of the bio-AgNPs (white bars) or chemical AgNPs (gray bars) in M9 buffer for 96 h at 20 °C. Data are presented as mean ± SEM. * indicates statistical significance based on ANOVA followed by Dunnett's test, *p < 0.05, **p < 0.01, ***p < 0.001, ****p < 0.0001.

depending on the volume and architecture of corona in biogenic NPs, doses could be adequately adjusted to achieve the most efficient biocide activity. Also, since the corona represents the way in which the cell recognizes the particle (Monopoli et al., 2012), deciphering the nature of the protein's arrangement in the surface of bio-NPs will lead us to understand NP-cell interaction.

The constituents of the surface coating associated with the bio-AgNPs were characterized. Protein electrophoresis technique was employed, and in both the cell-free filtrate and the capping removed from bio-AgNPs showed bands that were attributed to proteins responsible for synthesis and stabilization of the NPs (Fig. 3 and Supple Fig. 1). Also, under non-reducing conditions we detected lacasse activity for both the filtrate and the bio-AgNPs, suggesting the presence of active enzymes in the corona (Fig. 3). Chemical manufacture of NPs requires an additional step in the process in which polymers and/or surfactants are combined to adhere and cover the NP surface. This step is called functionalization, and it facilitates the anchoring of a substance on the NP external layer (Mout et al., 2012). Opposite, for bio-AgNPs synthesis no additional steps were required, since development of the outer layer took place simultaneously with biogenesis of the particle, through the biomolecules derived from the fungal exudates.

Several molecules were described to be involved in the NPs formation process, such as those associated with electron transfer during the conversion of Nicotinamide adenine dinucleotides like NADPH/NADH to NADP+/NAD+ (Gudikandula et al., 2017). NADH and NADH-dependent nitrate reductase enzymes are considered to be most important in the biogenic synthesis of metallic NPs (Baymiller et al., 2017). Biological molecules present in the fungal cell-free filtrate used in this paper, worked as a nanoscopic factory rendering bio-functionalized AgNPs capped with several macromolecules, many of them enzymes. Proteomic analysis of the bio-AgNPs showed that the hits detected correspond to *M. phaseolina* proteins (Fig. 4 and Table 1). We also identified secretion signal peptides in several enzymes, like amylases, peptidases, chitinase, and phosphatases that explain their presence in the aqueous cell-free filtrate (Table 1). Several enzymes involved in catalyzing oxide-reduction processes, in particular a multicopper oxidase with a signal peptide that could be a laccase (Table 1). Laccases (EC 1.10.3.2) are very versatile enzymes, extracellular glycoproteins described as oxidases that contain multi copper atoms, involved in the oxidation of phenolic and non-phenolic substrates with concomitant reduction of O_2 to H_2O (Mehra et al., 2018). In this case, some of these proteins might act together as redox groups collaborating to convert silver ions into metallic silver, but also those enzymes on the surface could retain activity to interact with cells. Furthermore, to obtain a long-life enzyme attached to the bio-NP rendering a stable catalyst will allow us to start studying tailored decoration of NP, to focus also on the lifetime of the enzymes and reutilization of the particle. Many groups are working on functionalizing NPs with active enzymes, first synthesizing the particles and functionalizing them in a later step. In this paper and with our current green methodology the synthesis and outer layer decoration in one step is achieved.

Currently, the focus is not only on tailoring NPs with pre-defined properties but also to develop nanomaterials with specific coatings to be used in medicine as carriers, like in cancer therapeutics and targeted drug-delivery (Erdogan et al., 2019; Gomes et al., 2021). In addition, the plasticity that nanotechnology nowadays offers allows us to be able to control surface charge and chemistry of the shell in NPs, as well as to design nanocomposites that release pre-loaded drugs or bioactive molecules at a specific site, surpassing low bioavailability and chemical instability problems (Krishnan et al., 2020).

Another interesting fact of green synthesis and decorating the outer layer in NPs is that the organic composition of the corona in the NPs masks the metallic core making it biocompatible (Mohanta et al., 2018). This event could induce the rate of internalization and retention of the biogenic particle inside the organisms. Thus, the nematode *C. elegans* was included to assess the inhibition of growth, reproduction, and fertility of the nematodes by exposure to different concentrations of the bio-AgNPs in comparison to the chemical AgNPs (Fig. 5). Remarkably, the three variables analyzed were affected by the presence of chemical AgNP in lower concentrations than with bio-AgNP, which suggests a greater toxicity of those of chemical origin. The body length and the percentage of gravid organisms of the worms that were exposed to the chemical AgNP in a concentration of 100 mg/L were negatively affected, while the worms treated with bio-AgNP did not show any effect under

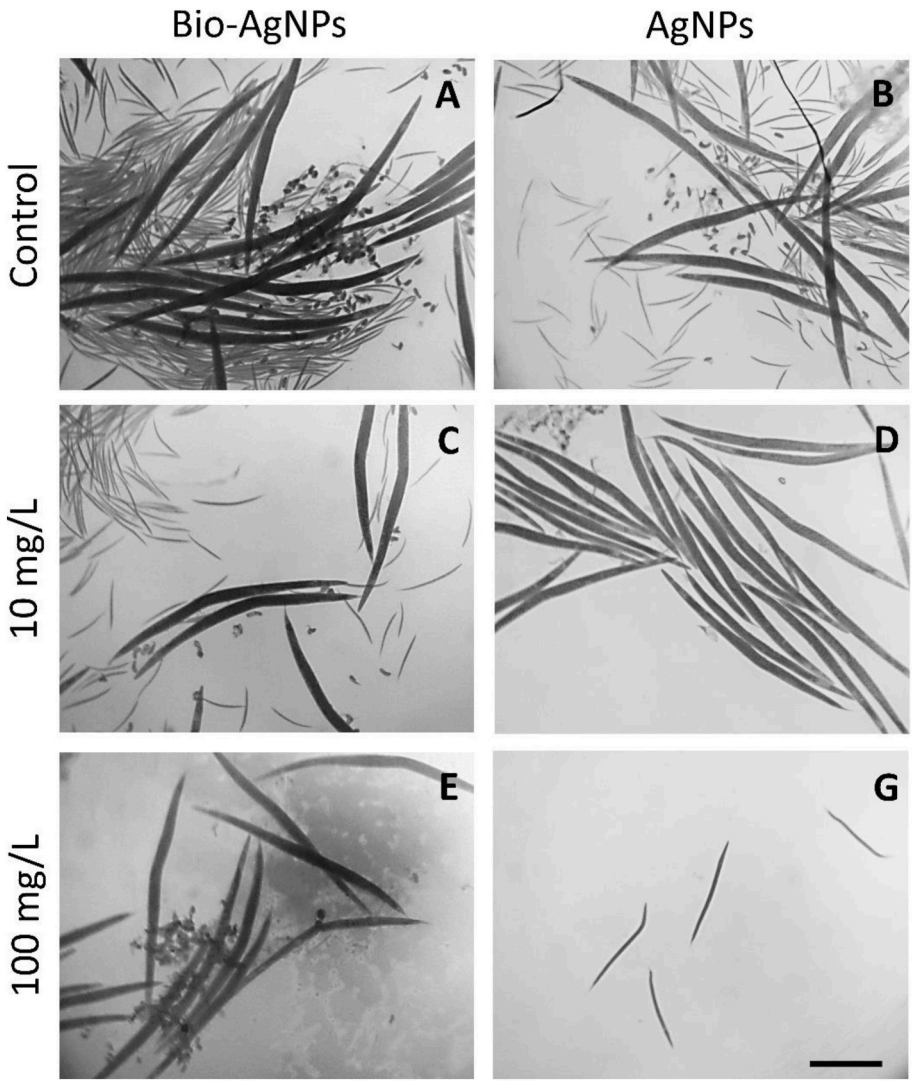

Fig. 6. Representative images of *C. elegans* length after exposure to concentrations of 0, 10 and 100 mg/L of the bio-AgNPs or chemical AgNPs in M9 buffer for 96 h at 20 °C (bar = 400 μm).

the concentrations tested (Figs. 5 and 6). Regarding reproduction, the treatment of nematodes with more than 10 mg/L of bio-AgNPs had an impact on the size of the offspring in comparison with the control group. However, with a ten-time smaller dose a significant decrease in the reproduction of nematodes treated with chemical AgNPs was observed (Fig. 5). Similar observations were made by Ranjani et al. (2021), who described comparable *C. elegans* survival rate when the worms were treated with green silver NPs synthetized by an endophytic fungus. Results from this study are in agreement with our research, suggesting that green NPs are less toxic to *C. elegans* than naked silver nanoparticles. Toxicological studies involving metallic NPs have already been published in organisms ranging from bacteria to humans (Marin et al., 2015). Although it is generally accepted that oxidation and subsequent release of Ag ions from the NPs is a major source of reactive oxygen species in a cell, the cause and mechanism triggering toxicity is still not fully understood, and almost no information on biogenic NPs is available.

The present study suggests that more emphasis should be given to the use of biological synthesis for commercial production of metallic NPs. The bio-AgNPs here studied showed to possess a capping derived from the fungal exudates, which confer stability, allowing storage. Conditional to the organism or biological constituents used to synthesize the particle, the outer layer of the NPs may also exhibit biological activity, acting concomitantly with the metallic NP core.

6. Conclusions

In the present study some of the positive aspects of synthesizing and using bio-AgNPs versus chemical AgNPs are showed. Green production of AgNPs in one step method using fungal cell-free filtrates as catalysts is a cost-efficient and environmentally friendly way to produce decorated metallic NPs. Results show that bio-AgNPs displayed high bactericidal

activity, while being more stable in time than chemical AgNPs, a feature that allows storage to handle and use deferred time. Through proteomic approach the organic composition of the corona in the bio-AgNPs was evaluated. Results suggest that the capping provides the unique features here described, like masking the metallic core making the bio-AgNPs less toxic to eukaryotes, and therefore biocompatible.

Credit author statement

Federico N. Spagnoletti: Conceptualization, Methodology, Writing-Original draft preparation. **Florencia Kronberg:** Visualization, Investigation. **Cecilia Spedalieri:** Supervision. **Eliana Munarriz:** Data curation, Resources. **Romina Giacometti:** Original idea, Writing-Reviewing and Editing, Funding acquisition.

Declaration of competing interest

The authors declare that they have no known competing financial interests or personal relationships that could have appeared to influence the work reported in this paper.

Acknowledgments

This study was supported by Consejo Nacional de Investigaciones Científicas y Técnicas (CONICET) and Agencia Nacional de Promoción Científica y Tecnológica (ANPCyT), PICT-2017-107 to RG. We thank Dr. Charalampos Panagos for his kind and careful corrections. The authors are very grateful for the insightful and helpful comments and constructive suggestions made by the anonymous Referees that have further improved this manuscript.

Appendix A. Supplementary data

Supplementary data to this article can be found online at https://doi.org/10.1016/j.jenvman.2021.113434.

References

Ahmad, S., Munir, S., Zeb, N., Ullah, A., Khan, B., Ali, J., Bilal, M., Omer, M., Alamzeb, S., Salman, S.M., Ali, S., 2019. Green nanotechnology: a review on green synthesis of silver nanoparticles - an ecofriendly approach. Int. J. nanomedicine. 14, 5087–5107. https://doi.org/10.2147/IJN.S200254.

Akther, T., Mathipi, V., Kumar, N.S., Davoodbasha, M., Srinivasan, H., 2019. Fungal-mediated synthesis of pharmaceutically active silver nanoparticles and anticancer property against A549 cells through apoptosis. Environ. Sci. Pollut. Res. 26, 13649–13657. https://doi.org/10.1007/s11356-019-04718-w.

Baas, J., Augustine, S., Marques, G.M., Dorne, J.L., 2018. Dynamic energy budget models in ecological risk assessment: from principles to applications. Sci. Total Environ. 628, 249–260. https://doi.org/10.1016/j.scitotenv.2018.02.058.

Bahrulolum, H., Nooraei, S., Javanshir, N., Tarrahimofrad, H., Mirbagheri, V.S., Easton, A.J., Ahmadian, G., 2021. Green synthesis of metal nanoparticles using microorganisms and their application in the agrifood sector. J. Nanobiotechnol. 19, 1–26. https://doi.org/10.1186/s12951-021-00834-3.

Ballottin, D., Fulaz, S., Souza, M.L., Corio, P., Rodrigues, A.G., Souza, A.O., Gaspari, P.M., Gomes, A.F., Gozzo, F., Tasic, L., 2016. Elucidating protein involvement in the stabilization of the biogenic silver nanoparticles. Nanoscale Res. Lett. 11, 1–9. https://doi.org/10.1186/s11671-016-1538-y.

Barwal, I., Ranjan, P., Kateriya, S., Yadav, S.C., 2011. Cellular oxido-reductive proteins of *Chlamydomonas reinhardtii* control the biosynthesis of silver nanoparticles. *J.* Nanobiotechnol. 9, 56. https://doi.org/10.1186/1477-3155-9-56.

Baymiller, M., Gobble, A., Huang, F., 2017. Rapid one-step synthesis of gold nanoparticles using the ubiquitous coenzyme NADH. Matters 3 (7), e201705000007. https://doi.org/10.19185/matters.201705000007.

Bradford, M.M., 1976. A rapid and sensitive method for the quantitation of microgram quantities of protein utilizing the principle of protein-dye binding. Anal. Biochem. 72, 248–254. https://doi.org/10.1006/abio.1976.9999.

Brenner, S., 1974. The genetics of *Caenorhabditis elegans*. Genetics 77, 71–94.

de Souza, T.A.J., Souza, L.R.R., Franchi, L.P., 2019. Silver nanoparticles: an integrated view of green synthesis methods, transformation in the environment, and toxicity. Ecotoxicol. Environ. Saf. 171, 691–700. https://doi.org/10.1016/j.ecoenv.2018.12.095.

Deepak, P. Umamaheshwaran, Guhan, K., Nanthini, R., Krithiga, B., Jaithoon, N., Gurunathan, S., 2011. Synthesis of gold and silver nanoparticles using purified URAK. Colloids Surf. B Biointerfaces 86, 353–358. https://doi.org/10.1016/j.colsurfb.2011.04.019.

Erdogan, O., Abbak, M., Demirbolat, G.M., Birtekocak, F., Aksel, M., Pasa, S., Cevik, O., 2019. Green synthesis of silver nanoparticles via *Cynara scolymus* leaf extracts: the characterization, anticancer potential with photodynamic therapy in MCF7 cells. PloS One 14 (6), e0216496. https://doi.org/10.1371/journal.pone.0216496.

Gomes, H.I., Martins, C.S., Prior, J.A., 2021. Silver nanoparticles as carriers of anticancer drugs for efficient target treatment of cancer cells. Nanomaterials 11 (4), 964. https://doi.org/10.3390/nano11040964.

Gong, P., Li, H., He, X., Wang, K., Hu, J., Tan, W., Tan, S., Zhang, X.Y., 2007. Preparation and antibacterial activity of Fe_3O_4@Ag nanoparticles. Nanotechnology 18, 604–611. https://doi.org/10.1088/0957-4484/18/28/285604.

Gudikandula, K., Vadapally, P., Charya, M.S., 2017. Biogenic synthesis of silver nanoparticles from white rot fungi: their characterization and antibacterial studies. Open 2, 64–78. https://doi.org/10.1016/j.onano.2017.07.002.

Gurunathan, S., Han, J.W., Kwon, D.N., Kim, J.H., 2014. Enhanced antibacterial and anti-biofilm activities of silver nanoparticles against Gram-negative and Gram-positive bacteria. Nanoscale Res. Lett. 9, 1–17. https://doi.org/10.1186/1556-276X-9-373.

Heukeshoven, J., Dernick, R., 1985. Simplified method for silver staining of proteins in polyacrylamide gels and the mechanism of silver staining. Electrophoresis 6, 103–112. https://doi.org/10.1002/elps.1150060302.

Höss, S., Nguyen, H.T., Menzel, R., Pagel-Wieder, S., Miethling-Graf, R., Tebbe, C.C., Jehle, J.A., Traunspurger, W., 2011. Assessing the risk posed to free-living soil nematodes by a genetically modified maize expressing the insecticidal Cry3Bb1 protein. Sci. Total Environ. 409, 2674–2684. https://doi.org/10.1016/j.scitotenv.2011.03.041.

Huang, J., Lin, L., Sun, D., Chen, H., Yang, D., Li, Q., 2015. Bio-inspired synthesis of metal nanomaterials and applications. Chem. Soc. Rev. 44, 6330–6374. https://doi.org/10.1039/C5CS00133A.

Hunt, P.R., Camacho, J.A., Sprando, R.L., 2020. *Caenorhabditis elegans* for predictive toxicology. Curr. Opin. Toxicol. 23, 23–28. https://doi.org/10.1016/j.cotox.2020.02.004.

Khan, N.T., Khan, M.J., Jameel, J., Jameel, N., Rheman, S.U.A., 2017. An overview: biological organisms that serves as nanofactories for metallic nanoparticles synthesis and fungi being the most appropriate. Bioceram. Dev. Appl. 7, 101. https://doi.org/10.4172/2090-5025.1000101.

Khoshnamvand, M., Huo, C., Liu, J., 2019. Silver nanoparticles synthesized using *Allium ampeloprasum* L. leaf extract: characterization and performance in catalytic reduction of 4-nitrophenol and antioxidant activity. J. Mol. Struct. 1175, 90–96. https://doi.org/10.1016/j.molstruc.2018.07.089.

Kim, J.S., Kuk, E., Yu, K.N., Kim, J.H., Park, S.J., Lee, H.J., Kim, S.H., Park, Y.K., Park, Y. H., Hwang, C.Y., Kim, Y.K., Lee, Y.S., Jeon, D.H., Cho, M.H., 2007. Antimicrobial effects of silver nanoparticles. Nanomedicine 3, 95–101. https://doi.org/10.1016/j.nano.2006.12.001.

Klimisch, H.J., Andreae, M., Tillmann, U., 1997. A systematic approach for evaluating the quality of experimental toxicological and ecotoxicological data. Regul. Toxicol. Pharmacol. 25, 1–5. https://doi.org/10.1006/rtph.1996.1076.

Krishnan, P.D., Banas, D., Durai, R.D., Kabanov, D., Hosnedlova, B., Kepinska, M., Fernandez, C., Ruttkay-Nedecky, B., Nguyen, H.V., Farid, A., Sochor, J., 2020. Silver nanomaterials for wound dressing applications. Pharmaceutics 12 (9), 821. https://doi.org/10.3390/pharmaceutics12090821.

Kumar, C.G., Poornachandra, Y., 2015. Biodirected synthesis of Miconazole-conjugated bacterial silver nanoparticles and their application as antifungal agents and drug delivery vehicles. Colloids Surf. B Biointerfaces 125, 110–119. https://doi.org/10.1016/j.colsurfb.2014.11.025.

Laemmli, U.K., 1970. Cleavage of structural proteins during the assembly of the head of bacteriophage T4. Nature 227, 680–685. https://doi.org/10.1038/227680a0.

Marambio-Jones, C., Hoek, E.V., 2010. A review of the antibacterial effects of silver nanomaterials and potential implications for human health and the environment. J. Nanoparticle Res. 12, 1531–1551. https://doi.org/10.1007/s11051-010-9900-y.

Marin, S., Mihail Vlasceanu, G., Elena Tiplea, R., Raluca Bucur, I., Lemnaru, M., Minodora Marin, M., Mihai Grumezescu, A., 2015. Applications and toxicity of silver nanoparticles: a recent review. Curr. Top. Med. Chem. 15, 1596–1604. https://doi.org/10.2174/1568026615666150414142209.

Mehra, R., Muschiol, J., Meyer, A.S., Kepp, K.P., 2018. A structural-chemical explanation of fungal laccase activity. Sci. Rep. 8, 17285. https://doi.org/10.1038/s41598-018-35633-8.

Mishra, S., Yang, X., Singh, H.B., 2020. Evidence for positive response of soil bacterial community structure and functions to biosynthesized silver nanoparticles: an approach to conquer nanotoxicity? J. Environ. Manag. 253, 109584. https://doi.org/10.1016/j.jenvman.2019.109584.

Mohamed, A.A., Fouda, A., Abdel-Rahman, M.A., Hassan, S.E.D., El-Gamal, M.S., Salem, S.S., Shaheen, T.I., 2019. Fungal strain impacts the shape, bioactivity and multifunctional properties of green synthesized zinc oxide nanoparticles. Biocatal. Agric. Biotechnol. 19, 101103. https://doi.org/10.1016/j.bcab.2019.101103.

Mohanta, Y.K., Nayak, D., Biswas, K., Singdevsachan, S.K., Abd_Allah, E.F., Hashem, A., Alqarawi, A.A., Yadav, D., Mohanta, T.K., 2018. Silver nanoparticles synthesized using wild mushroom show potential antimicrobial activities against food borne pathogens. Molecules 23 (3), 655. https://doi.org/10.3390/molecules23030655.

Monopoli, M.P., Åberg, C., Salvati, A., Dawson, K.A., 2012. Biomolecular coronas provide the biological identity of nanosized materials. Nat. Nanotechnol. 7, 779–786. https://doi.org/10.1038/nnano.2012.207.

Mout, R., Moyano, D.F., Rana, S., Rotello, V.M., 2012. Surface functionalization of nanoparticles for nanomedicine. Chem. Soc. Rev. 41, 2539–2544. https://doi.org/10.1039/c2cs15294k.

Mulfinger, L., Solomon, S.D., Bahadory, M., Jeyarajasingam, A.V., Rutkowsky, S.A., Boritz, C., 2007. Synthesis and study of silver nanoparticles. J. Chem. Educ. 84 (2), 322. https://doi.org/10.1021/ed084p322.

Piccinni, F.E., Ontañon, O.M., Ghio, S., Sauka, D.H., Talia, P.M., Rivarola, M.L., Valacco, M.P., Campos, E., 2019. Secretome profile of *Cellulomonas* sp. B6 growing on lignocellulosic substrates. J. Appl. Microbiol. 126, 811–825. https://doi.org/10.1111/jam.14176.

Prajapati, A.K., Mondal, M.K., 2021. Novel green strategy for CuO–ZnO–C nanocomposites fabrication using marigold (Tagetes spp.) flower petals extract with and without CTAB treatment for adsorption of Cr (VI) and Congo red dye. J. Environ. Manag. 290, 112615. https://doi.org/10.1016/j.jenvman.2021.112615.

Quinteros, M.A., Bonilla, J.O., Alborés, S.V., Villegas, L.B., Páez, P.L., 2019. Biogenic nanoparticles: synthesis, stability and biocompatibility mediated by proteins of *Pseudomonas aeruginosa*. Colloids Surf. B Biointerfaces 184, 110517. https://doi.org/10.1016/j.colsurfb.2019.110517.

Ranjani, S., Ahmed, M.S., MubarakAli, D., Ramachandran, C., Kumar, N.S., Hemalatha, S., 2021. Toxicity assessment of silver nanoparticles synthesized using endophytic fungi against nosacomial infection. Inorg. Nano-Met. Chem. 51, 1080–1085. https://doi.org/10.1080/24701556.2020.1814332.

Ruttkay-Nedecky, B., Skalickova, S., Kepinska, M., Cihalova, K., Docekalova, M., Stankova, M., Uhlirova, D., Fernandez, C., Sochor, J., Milnerowicz, H., Beklova, M., 2019. Development of new silver nanoparticles suitable for materials with antimicrobial properties. J. Nanosci. Nanotechnol. 19 (5), 2762–2769. https://doi.org/10.1166/jnn.2019.15867.

Salam, H.A., Sivaraj, R., Venckatesh, R., 2014. Green synthesis and characterization of zinc oxide nanoparticles from *Ocimum basilicum* L. var. *purpurascens* Bent. -Lamiaceae leaf extract. Mater. Llett. 131, 16–18. https://doi.org/10.1016/j.matlet.2014.05.033.

Schneider, C.A., Rasband, W.S., Eliceiri, K.W., 2012. NIH Image to ImageJ: 25 years of image analysis. Nat. Methods 9, 671–675. https://doi.org/10.1038/nmeth.2089.

Schröfel, A., Kratošová, G., Šafařík, I., Šafaříková, M., Raška, I., Shor, L.M., 2014. Applications of biosynthesized metallic nanoparticles–a review. Acta Biomater. 10, 4023–4042. https://doi.org/10.1016/j.actbio.2014.05.022.

Singh, P., Kim, Y.J., Zhang, D., Yang, D.C., 2016. Biological synthesis of nanoparticles from plants and microorganisms. Trends Biotechnol. 34, 588–599. https://doi.org/10.1016/j.tibtech.2016.02.006.

Spagnoletti, F.N., Spedalieri, C., Kronberg, F., Giacometti, R., 2019. Extracellular biosynthesis of bactericidal Ag/AgCl nanoparticles for crop protection using the fungus *Macrophomina phaseolina*. J. Environ. Manag. 231, 457–466. https://doi.org/10.1016/j.jenvman.2018.10.081.

Stiernagle, T., 2006. Maintenance of *C. elegans*. https://doi.org/10.1895/wormbook.1.101.1. WormBook 1-11.

Toledo, M.A., Santos, C.A., Mendes, J.S., Pelloso, A.C., Beloti, L.L., Crucello, A., Favaloro, M.T.P., Santiago, A.S., Schneideir, D.R.S., Saraiva, A.M., Stach-Machado, D.R., Souza, A.A., Trivella, D.B.B., Aparicio, R., Tasic, L., Azzoni, A.R., 2013. Small-angle X-ray scattering and in silico modeling approaches for the accurate functional annotation of an LysR-type transcriptional regulator. BBA-Proteins Proteom 1834, 697–707. https://doi.org/10.1016/j.bbapap.2012.12.017.

Wu, T., Xu, H., Liang, X., Tang, M., 2019. *Caenorhabditis elegans* as a complete model organism for biosafety assessments of nanoparticles. Chemosphere 221, 708–726. https://doi.org/10.1016/j.chemosphere.2019.01.021.

Xiao, C., Li, H., Zhao, Y., Zhang, X., Wang, X., 2020. Green synthesis of iron nanoparticle by tea extract (polyphenols) and its selective removal of cationic dyes. J. Environ. Manag. 275, 111262. https://doi.org/10.1016/j.jenvman.2020.111262.